IN-SITU MONITORING OF WATER INFILTRATION RECHARGE IN LARGE DEPTH IRRIGATION AREA UNDER PLANTING CONDITIONS

WANG, Y. Y.[1,2] – LI, Z. P.[1] – ZHAO, J.[1] – HE, Y. J.[2,3*]

[1]*College of Geosciences and Engineering, North China University of Water Resources and Electric Power, 450045, Zhengzhou, China*

[2]*The Institute of Hydrogeology and Environmental Geology, Chinese Academy of Geological Science, 050061, Shijiazhuang, China*

[3]*Geothermal and Hot Dry Rock Exploration and Development Technology Innovation Center, Ministry of Natural Resource, 050061, Shijiazhuang, China*

**Corresponding author*
e-mail: heyujiang86@163.com; phone: +86-132-9831-2790

(Received 3rd Mar 2022; accepted 20th Jun 2022)

Abstract. To explore the recharge characteristics of soil water infiltration in the large buried irrigation system, in-situ monitoring tests were performed at the Comprehensive Agricultural Experiment Station in the pre-mountain area of the North China Plain. The agro-meteorological monitoring system was used to monitor meteorological elements such as precipitation and evaporation in the irrigation area, and the water content and water potential of typical soil profiles were measured in-situ using the neutron probe and negative pressure meter. The groundwater level was monitored using a groundwater level recorder. The study analyzed the water infiltration process in different growth stages of crops and elucidated water dynamics under heavy precipitation conditions. Therefore, the multi-year water balance of the study area was determined by defining the potential infiltration recharge boundary. The results showed that the types of soil water movement at different growth stages differed significantly, while the water potential profile showed the same trend on the time scale. The effect of Rainfall on soil water transport has a lagging effect, with precipitation greater than 10 mm recharging soil water to a certain extent. The main sources of water recharge for the large buried soil layer under planting conditions were rainfall (55.68%) and irrigation (44.32%) and the main source of discharge was evapotranspiration (97.89%), with very little recharge (2.11%) to groundwater. These findings identified the characteristics of water circulation in irrigation areas with large burial depths.
Keywords: *North China Plain, soil water, time scale, potential groundwater recharge, water balance*

Introduction

The groundwater level has been declining due to the severe overdraft in the North China Plain, resulting in a serious imbalance in groundwater recharge and discharge and triggering geological problems such as the formation of a large cone of groundwater depression and the downward shift of the salt and freshwater interface (Lu et al., 2021). These significant changes in groundwater recharge and discharge, especially in the North China irrigation area, result in substantial inconsistencies in agricultural water supply and demand. Scholars have observed that understanding the soil water supply, water dynamic evolution mechanisms, soil nutrient and pollution transport processes, and regional water resource potential characteristics are essential to address water shortage issues in the agricultural areas of the North China Plain (Adhikari and Wang, 2020; Kassaye et al., 2019). However, the dynamic evolutionary pattern of soil water infiltration recharge, which is the core of the above-mentioned problem, remains unclear (Jia et al., 2019), particularly under human cropping conditions when the process is more complex.

http://www.aloki.hu ● ISSN 1589 1623 (Print) ● ISSN 1785 0037 (Online)
DOI: http://dx.doi.org/10.15666/aeer/2004_36313653

The soil water infiltration process is affected by various factors such as rainfall conditions, soil properties, crop coverage, and soil depth (Huang et al., 2021; Kamal et al.,2021). Soil water movement can be classified into four basic types: evaporation, infiltration, evaporation-infiltration, and infiltration-evaporation (Han et al., 2005). The analysis of soil water transport patterns is an important guide for water resource management in the North China Plains (Pereira et al., 2020). Pei et al. (2020) used a water cycle simulation of field experiments in large groundwater depth areas to quantify groundwater recharge and phreatic water supply. Zhang et al. (2020) and Pullens et al. (2021) studied the characteristics of soil water migration during the crop growth period by establishing a coupling model between hydrology and crop growth. Understanding the process of farmland water infiltration is essential for developing scientifically sound irrigation systems, planning and management of agricultural water resources, water-saving practices, and environmental assessment in major agricultural producing areas. Precipitation and irrigation are the primary sources of agricultural water recharge. The water content of the soil layer changes in a certain pattern because of external factors such as precipitation and irrigation, which affects the water absorption pattern, growth condition, distribution pattern of crops, and groundwater level (Zhang et al., 2007). The evolutionary mechanism of soil water movement after rainfall provides some guidance for crop irrigation mechanisms (Joly et al., 2019; Ayantobo et al., 2019). Researchers have experimentally verified that soil water transport has a certain lag after heavy precipitation (Kristo et al., 2019; Dias et al., 2021). Vermeire and Rinella (2020) studied the effects of seasonal rainfall on soil moisture and annual net primary production in a variety of plant combinations and observed that rainfall had no significant effect on soil moisture at 15–30 cm depth. Previous studies have scientifically evaluated soil water infiltration and soil-water environment dynamics in agricultural soils, which provide a foundation for this study (Xiao et al., 2021; Muhammad et al., 2021; Xu et al., 2021). However, the recharge characteristics of potential soil water infiltration under deep groundwater burial conditions and the influence of long-term precipitation were not considered, it is difficult to study the water regulation in the agricultural irrigation area of the deep vadose zone in North China that exhibits a large funnel area.

In this study, the Luancheng Agro-Ecosystem Experimental Station of the Chinese Academy of Sciences (32–48 m groundwater depth) was selected to conduct in-situ monitoring experiments for three consecutive years under summer maize and winter wheat. By observing the recharge characteristics of soil water under crop growth conditions, multiple growth stages and time scales, exploring the characteristics of precipitation impact in irrigation areas, defining the potential groundwater infiltration boundary to calculate the potential groundwater infiltration recharge in irrigation areas, and exploring the water balance characteristics of irrigation areas. It can provide reference indicators for the development of irrigation systems for farmland in the groundwater overdraft area of the North China Plain.

Materials and methods

Overview of the study area

The research site is located in Luancheng County, Shijiazhuang City (114°40′58″N, 37°53′16″E) in the middle of the piedmont Taihang Mountains in the North China plain. With a total area of 345 km^2 and 214 km^2 of arable land, this region is one of the main grain-producing regions in China (*Fig. 1*). The main crops of Winter Wheat and Summer Maize

http://www.aloki.hu ● ISSN 1589 1623 (Print) ● ISSN 1785 0037 (Online)
DOI: http://dx.doi.org/10.15666/aeer/2004_36313653

are rotated (Hu et al., 2021, 2006; Shen et al., 2021) and planted every year in an area of 164 km^2 and 127 km^2, respectively, and the annual output is sufficient to supply the local area and export. The tillage method in this study is tillage cultivation. It has a sub-humid climate in the warm temperate zone, with an annual mean temperature of 12.8 ℃ and annual precipitation of 474.0 mm. The thickness of the vadose zone goes up to 30 m, and the infiltration of rainfall and irrigation water recharges the groundwater all year round (Wei et al., 2017; Ju et al., 2016). The dynamics of shallow soil water are less affected by the dynamics of the groundwater level. The main focus of the study was the soil water dynamics in the unsaturated zone above 3.4 m. The soil was mainly composed of clay, silt, fine sand, and medium sand. The study area is located on an alluvial fan in front of the Taihang Mountains. The groundwater recharge, runoff, and drainage conditions were good. The general runoff direction is from northwest to southeast and from shallow to deep runoff.

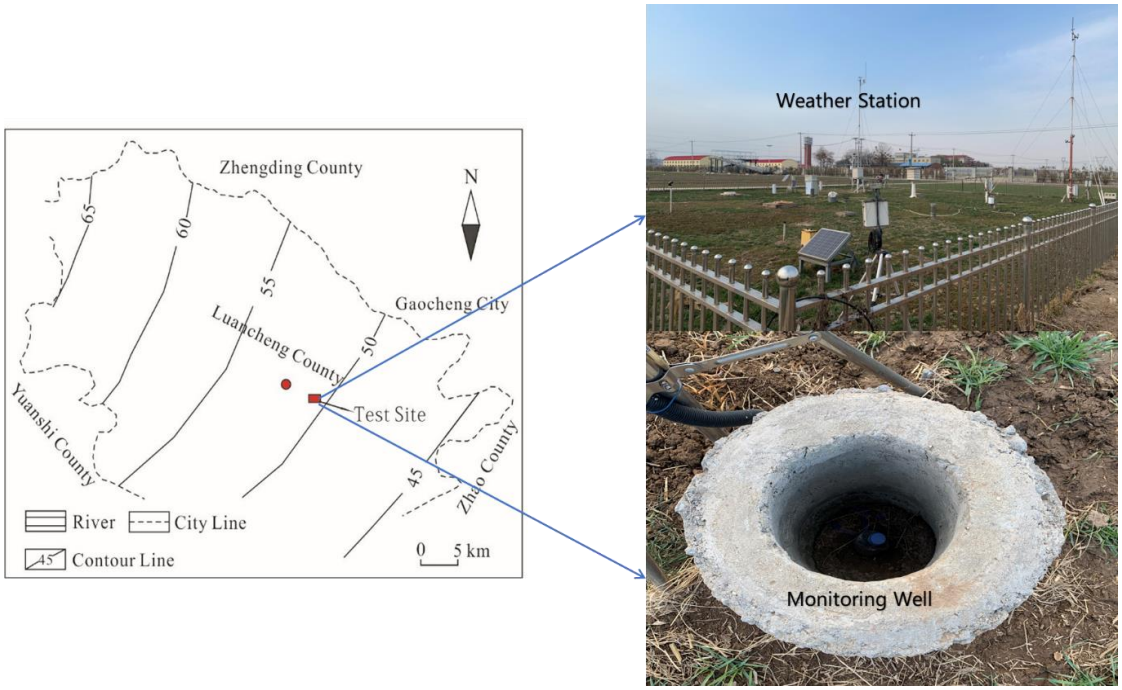

Figure 1. *Contour and regional location map of the study area (the experimental site is located in the Taihang Mountain Front Plain, within the Agricultural Experimental Station of the Chinese Academy of Sciences, Luancheng County, Shijiazhuang City, Hebei Province, China)*

Data

In-situ monitoring

The research site was equipped with monitoring systems that included negative pressure meters and neutron probes for monitoring soil water potential, groundwater level, and meteorological factors at the site. The neutron probes were calibrated in layers before the start of the test. Each monitoring system had 20 negative pressure meters and 20 neutron probes buried at depths of up to 340 cm. One negative pressure meter and one neutron probe were installed every 10 cm within the first 100 cm of depth, every 20 cm between 100–260 cm of depth, and every 40 cm between 260–340 cm of depth. The installation method was a buried oblique plug type. The Diver groundwater level recorder was used to monitor the changes in the groundwater level at the test site. In addition, there was a standard weather

http://www.aloki.hu ● ISSN 1589 1623 (Print) ● ISSN 1785 0037 (Online)
DOI: http://dx.doi.org/10.15666/aeer/2004_36313653

station approximately 50 m away from the test field, which monitors rainfall, evaporation, and other parameters. The irrigation amount was determined according to the actual irrigation amount recorded by the field water meter. The irrigation method was broad irrigation. Some meteorological monitoring data in continuous monitoring years are shown in *Figure 2*, in which the E20 evaporator measures the water surface evaporation. Other meteorological data needed in the study are provided by the National Tibetan Plateau Data Center (http://data.tpdc.ac.cn), mainly for daily maximum temperature, daily minimum temperature, daily average temperature, wind speed and sunshine hours.

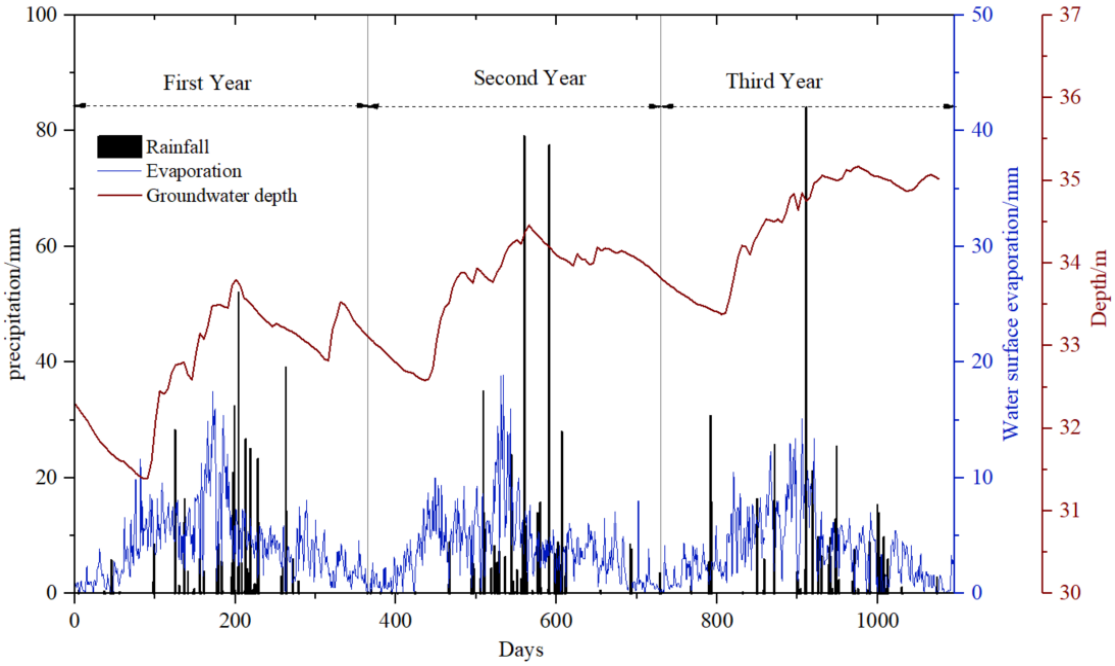

Figure 2. *Meteorological conditions during the monitoring period in the Luancheng area (including groundwater levels, daily evaporation, and daily rainfall)*

Field monitoring was carried out in three stages, with each stage lasting one year, from 2005-2007. The data on soil suction and moisture content were collected during the growth period of wheat and maize for three consecutive years. Monitoring frequencies are shown in *Table 1*. Precipitation or irrigation during the monitoring intensified the observations. Generally, the data were collected once in the first hour and then every 2–4 h, and the time interval was gradually extended until the regular observation time was restored.

Table 1. *Monitoring items, instrumentation and frequency*

Monitoring program	Instrument	Monitoring frequency
Groundwater level	Groundwater level automatic monitor Diver	Every 5 days
Moisture content	CNC503DR Neutron Probe	Every 3 days
Soil water potential	WM-1 mercury type negative pressure gauge system	Every 3 days
Meteorological data (rainfall, evaporation, etc.)	Rain gauge, E20 evaporator, etc.	Everyday

http://www.aloki.hu ● ISSN 1589 1623 (Print) ● ISSN 1785 0037 (Online)
DOI: http://dx.doi.org/10.15666/aeer/2004_36313653

Methods

(1) Soil water potential measurements

A negative pressure meter is suitable for measuring soil moisture in irrigated farmlands and soils with high moisture content when used with a soil moisture meter. However, studying the soil water movement mechanism is essential for the development of an instrument. In this study, the soil water potential measurement was based on the reading of the mercury manometer, which can be derived from the negative soil pressure. As shown in *Equation* 1 (Li et al., 2014):

$$\Psi_m = -12.6H_1 + 13.6H_0 - H_a + Z \quad \text{(Eq.1)}$$

where Ψ_m is the negative soil pressure; H_1 is the height of the mercury level in the negative pressure meter; H_0 is the height of the mercury level in the mercury meter; H_a is the distance between the zero scales of the observation plate and the ground surface; and Z is the vertical distance between the center position of the clay head and the ground surface. The negative pressure meter H_a of the test point in this study is 133.5 cm.

The soil water potential was calculated using the observation data of the negative pressure meter to obtain the distribution curve of the soil water potential and subsequently determine the zero-flux surface. The zero-flux surface was used to analyze the soil water characteristics under different conditions and explore the effects of precipitation, irrigation infiltration, evaporation, and plant root water absorption on soil water movement.

(2) Potential infiltration recharge of groundwater

The maximum depth associated with zero flux downward development in the North China Plain can be evaluated in areas with substantial water level burial depth. Calculating the water flux of a specific boundary in the slowly changing gradient zone of soil water potential below the deepest zero flux surface, together with the soil water flux of that boundary, is equivalent to determining the vertical infiltration recharge of precipitation or irrigation water. The calculation of soil water flux *Q* at the location boundary *Z* must match with the water potential data near the location boundary *Z* and measure the unsaturated hydraulic conductivity $K(\theta)$ or $K(\psi_m)$. First, according to the soil water potential data, the calculated period was divided into *n* hours, and the soil water flux at the positioning boundary in each hour was calculated using Darcy's law. Then, the soil water flux for each hour was aggregated to obtain the soil water quantity passing through the positioning boundary in the calculation period (Jing et al., 1994). As shown in *Equation 2*.

$$Q_{(Z)} = -\sum_{i=1}^{n} K(\theta_i) \cdot \left(\frac{\Delta \psi}{\Delta z} \right) \cdot (\Delta t)_i, \quad i = 1, 2, \cdots, n \quad \text{(Eq.2)}$$

where $Q_{(Z)}$ is the amount of soil water passing from the localized boundary *Z*; θ_i and $\frac{\Delta \psi}{\Delta z}$ are the average soil water content and average soil water potential gradient at the

http://www.aloki.hu ● ISSN 1589 1623 (Print) ● ISSN 1785 0037 (Online)
DOI: http://dx.doi.org/10.15666/aeer/2004_36313653

positioning boundary Z in the ith period, respectively; $K(\theta_i)$ is the unsaturated hydraulic conductivity when the average value of soil water content is in the ith time period; and $(\Delta t)_i$ is the ith hourly period.

The key to calculating the infiltration recharge using this method is the determination of the unsaturated hydraulic conductivity $K(\theta_i)$. The zero flux plane method was used to determine the unsaturated hydraulic conductivity $K(\theta)$ of the soil using Darcy's law, as shown in *Equation 3.*

$$q(z) = -K(\theta)\frac{\partial \psi}{\partial z} \text{ or } q(z) = -K(\psi_m)\frac{\partial \psi}{\partial z} \quad \text{(Eq.3)}$$

This equation can be rearranged as:

$$K(\theta) = -q(z) / \frac{\partial \psi}{\partial z} \text{ or } K(\psi_m) = -q(z) / \frac{\partial \psi}{\partial z} \quad \text{(Eq.4)}$$

where θ, ψ, and $\frac{\partial \psi}{\partial z}$ are the average values of soil water content, matric potential, and soil water potential gradient at the positioning boundary Z from time period t_1 to t_2, respectively. During the effective period of the zero-flux surface, the position $z_0(t_1)$ and $z_0(t_2)$ of the ZFP can be determined by the water content and water potential distribution at t_1 and t_2. The ZFP method was used to calculate the water quantity D at Z from t_1 to t_2. $D = \int_{z_0}^{z} \theta(z,t_1)dz - \int_{z_0}^{z} \theta(z,t_2)dz$. The soil water flux was obtained from the equation $q(z) = D / \Delta t(\Delta t = t_1 - t_2)$. The value of unsaturated hydraulic conductivity was derived based on *Equation 4.*

(3) Evapotranspiration

Rooting depths range from 0 to 200 cm for maize and 0 to 60 cm for wheat (Ordóñez et al., 2018; Li et al., 2022). Considering the different cropping patterns in the monitoring year, the evapotranspiration ET for the different cropping patterns is divided into evapotranspiration from the crop and evaporation from the soil in the no-crop period. Crop transpiration under standard conditions is calculated using *Equation 5.*

$$ET_c = ET_0 \times K_c \quad \text{(Eq.5)}$$

where: ET_c is the crop transpiration (mm/d); ET_0 is the reference crop transpiration (mm/d); $K_{c\text{end}}$ is the crop coefficient, determined according to the FAO56 recommended crop coefficient (Allen et al., 1998). The crop coefficients were divided into initial growth period $K_{c\text{ini}}$, middle growth period $K_{c\text{mid}}$ and maturity period $K_{c\text{end}}$, where the growth coefficients were 0.3, 1.2 and 0.4 for maize and 0.4, 1.15 and 0.3 for wheat.

http://www.aloki.hu ● ISSN 1589 1623 (Print) ● ISSN 1785 0037 (Online)
DOI: http://dx.doi.org/10.15666/aeer/2004_36313653

The daily evapotranspiration of the reference crop was calculated using the Penman-Monteith *Equation 6.*

$$ET_0 = \frac{0.408\Delta(R_n - G) + r\frac{900}{T+273}u_2(e_s - e_a)}{\Delta + r(1 + 0.34u_2)} \quad \text{(Eq.6)}$$

where R_n is the net radiation of canopy surface (MJ/(m^2·d)); G is soil heat flux (MJ/(m^2·d)); Δ is the slope of the relationship curve between saturated water vapor pressure and air temperature (kPa/°C); T is the mean daily temperature (°C) at 2 m; r is a constant of the hygrometer (kPa/°C); u_2 is a hygrometer constant (kPa/°C); e_s is saturated water pressure (kPa); e_a is the actual water pressure (kPa).

The E20 evaporator dish in the study measured the evaporation from the water surface, and the ET_s of evaporation from the soil surface can be found by converting *Equation 7.*

$$ET_s = \alpha \times E_{20} \quad \text{(Eq.7)}$$

where ET_s is the Soil surface evaporation (mm*a-1); α is an empirical coefficient, here taken as 0.54 (Wang et al., 2005); E_{20} is the E20 evaporator reading (mm*a-1).

(4) Water balance

The water balance method involves the systematic use of meteorological, plant growth, and farmland irrigation data. The infiltration recharge (Q) of soil water from the surface to the soil, without considering lateral runoff, can be estimated with the help of *Equation 8* (Li et al., 2017).

$$Q = P + I - E_T - \Delta W \quad \text{(Eq.8)}$$

where E_T is the evapotranspiration (mm*a-1); E_{20} is the E20 evaporator reading (mm*a-1); Q is the soil moisture flux at the locus boundary (mm; positive upward and negative downward); P is the rainfall (mm); I is the irrigation (mm); E_T is the evapotranspiration (mm), including soil surface evaporation and crop transpiration; and ΔW is the soil water storage variable (negative for the increase and positive for decrease), which can be determined by measuring the water content distribution in the soil profile.

Results

Soil moisture movement under planting conditions

Water infiltration pattern during the complete crop growth period

The soil water potential at different depths during the crop growth period was analyzed and its variation with time was plotted (*Fig. 3*). By comparing the soil

http://www.aloki.hu ● ISSN 1589 1623 (Print) ● ISSN 1785 0037 (Online)
DOI: http://dx.doi.org/10.15666/aeer/2004_36313653

moisture movement curves and rainfall at different depths during the complete growth period of maize (*Fig. 3 a, b,* and *c*) and wheat (*Fig. 3 e, f,* and *g*), it was observed that the distribution of water potential in the soil has noticeable zoning characteristics. The shallow soil (0–100 cm), which is a zone that exhibits a significant change in soil water potential, is susceptible to rainfall infiltration recharge, evaporation, and transpiration. The downward movement of soil water to the lower layers of soil is caused by precipitation and irrigation. Moreover, the upward movement of water, which has been generally used for crop growth or to recharge the atmosphere, is caused by evaporation, transpiration, root water uptake, and other functions. The soil layer between 100–200 cm depth, which represents the lag zone of soil water potential change, is affected by external influences and causes a change in the soil water movement state. Based on the change in soil water movement during the growth period of maize, it was observed that the changing trend of soil water potential gradually slowed over time, and the overall trend of water movement was stable. However, the water potential during the wheat growth period was stable up to 175 days and changed significantly after 175 days, indicating that the change in soil moisture movement was lagging by external factors during this period. The soil layer between 200–300 cm depth, which represents the zone that exhibits a stable soil water potential change, was less affected by external precipitation and evaporation; the soil water potential and water movement were relatively stable. The soil layer below the depth of 300 cm, which is a zone exhibiting deep soil water movement, was not affected by external factors such as precipitation and irrigation; however, the soil water potential changed significantly with time. The reason for this phenomenon may be the groundwater level or the effect of the dominant flow of large channels.

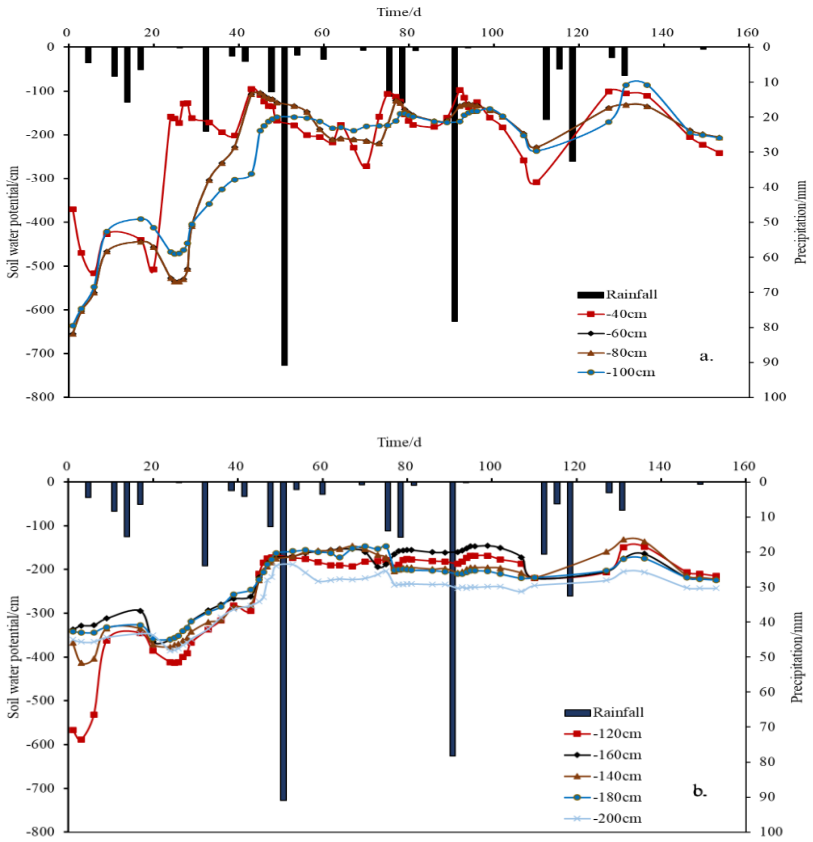

http://www.aloki.hu ● ISSN 1589 1623 (Print) ● ISSN 1785 0037 (Online)
DOI: http://dx.doi.org/10.15666/aeer/2004_36313653

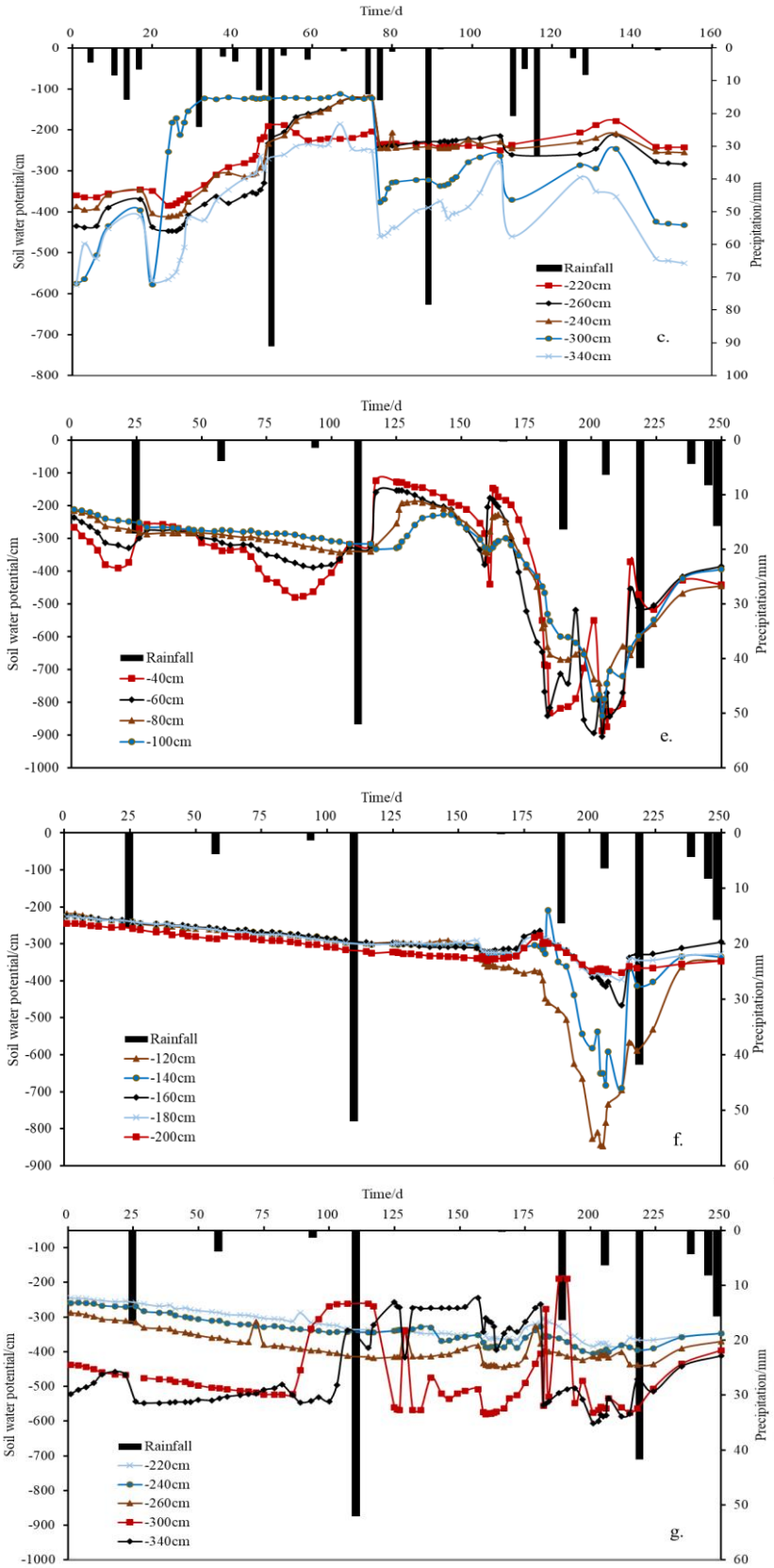

Figure 3. *Soil water movement at different depths during the complete growth period of maize and wheat. a, b, and c are the changes of soil water movement at different depths of maize; e, f, g are the changes of soil water movement at different depths of wheat*

http://www.aloki.hu ● ISSN 1589 1623 (Print) ● ISSN 1785 0037 (Online)
DOI: http://dx.doi.org/10.15666/aeer/2004_36313653

Variation characteristics of soil water infiltration changes at different crop growth stages

In this study, we selected water potential change curves of two crops during their growth period (summer maize and winter wheat) to explore the soil water transport patterns in the study area. Subsequently, the second stage of the growth period of maize and wheat was selected for the study. Furthermore, the growth period of summer maize was divided into emergence, jointing, flaring, booting, and maturation stages. It was observed that the soil water potential of summer maize varies significantly at different growth stages (*Fig. 4a*). The soil water movement at the emergence and jointing stages was the evaporation-infiltration type, which may be affected by rainfall or irrigation. There is a polymeric zero-flux surface at 80–100 cm depths. The variation trend of the soil water potential was stable. The peak of the emergence stage was noted at a burial depth of 80 cm when the soil water potential reached -527.48 cm. The peak water potential at the same depth of the jointing stage was -107.96 cm, and the overall upward movement of soil moisture may be accounted for by the strong evaporation and high water demand at the early growth stage; thus, soil moisture was more affected.

The water potential difference at different depth ranges in the middle and later stages of maize growth narrowed under the influence of precipitation, evaporation, and other external conditions, and the trend of soil water potential change showed a relative flatness. There were several small zero-flux surfaces in the flaring stage, the soil water movement type was mainly evaporation-infiltration type, and soil water moved downward to supply the soil layer. The soil water potential was minimal at a depth of 140 cm during the emergence and jointing stages, and the water showed a trend of downward infiltration. The variation in soil water potential during the booting and maturation stages was relatively lower, and the soil water movement type was mainly of the infiltration type, with the zero-flux surface being positioned between 100–120 cm depth. The overall water potential gradually increased with an increase in the burial depth of the profile, and the overall soil water was in a downward movement state; however, at shallow depths, the soil water exhibited an upward movement.

The growth period of winter wheat was divided into emergence, overwintering, returning green, jointing, filling, and maturation stages. It can be seen from *Figure 4b* that the characteristics of the total water potential curves in the soil profile at each growth stage of wheat. The evaporation intensity was low during the emergence, overwintering, and returning green stages because of lower temperatures and rainfall in winter and early spring, and the soil water movement type of the three curves is the evaporation-infiltration type. The water potential was ~~clearly~~ inflected at a burial depth of 260 cm when soil moisture was recharged downward to groundwater. At the emergence and overwintering stages, the location of the zero-flux surface was at a burial depth of 80–100 cm. Small polymeric zero-flux surfaces existed near the ground during the returning green period. This phenomenon is observed due to the snow cover on the surface in winter, which melts in ~~the~~ warm weather and reduces ~~the~~ evapotranspiration; therefore, the soil moisture infiltrates downward near the surface. The soil water potential changes significantly during the jointing, filling, and maturation stages, and the soil water movement type is mainly infiltration. In the jointing period, there is a very large value at a burial depth of 50 cm, which is the location of the dispersion-type zero-flux surface where the upper part evaporates and

http://www.aloki.hu ● ISSN 1589 1623 (Print) ● ISSN 1785 0037 (Online)
DOI: http://dx.doi.org/10.15666/aeer/2004_36313653

the lower part infiltrates; there is a high soil water potential point in the middle. At the filling and maturation stages, there is a very small value of soil water potential near the surface, and there is a polymeric type zero flux surface, which may be influenced by irrigation.

By analyzing the changes in the type of water movement during the crop growing period, it was shown that precipitation, irrigation, evaporation, and plant root uptake had significant effects on the type of soil water movement. During the growing period of summer corn, precipitation and irrigation were greater, evaporation was more intense, crop water demand was large, root uptake was stronger, and soil water movement was more complex. During the growth period of winter wheat, owing to the low temperature and low precipitation, soil water evaporation and root water absorption capability are weak. The soil moisture in the middle and late growth periods of wheat moves downward with the warming of temperature, which is affected by precipitation and irrigation.

Soil profile water transport variation rules on time scale

To demonstrate the trend of soil water potential overtime during the crop growth period, we selected three years of comparative soil water potential movement before and after the same growth stage of maize, with three growth stages: emergence, flaring, and maturation. From the soil water potential profile (*Fig. 5*), it was observed that the soil water potential of maize in the emergence stage (*Fig. 5a*) changed more significantly, and the type of soil water movement was complex for three consecutive years. The water potential of maize at the emergence stage showed multiple changes within the burial depth of 80–160 cm, which was significantly influenced by external factors such as precipitation, irrigation, and root water uptake. At the flaring stage (*Fig. 5b*), the soil water potential changes more gently. The soil water movement type is simple and stable for three consecutive years, showing an evaporation-based movement state. At the maturation stage (*Fig. 5c*), the soil water potential showed an inflection point, and the soil water potential was similar in the second and third years, and was significantly lower in the first year. This shows that the soil water content was significantly lower in the first year of maize maturity when the soil was subject to strong evaporation or less rainfall and other factors, as compared to that in the remaining two years. However, the trend of soil water potential change was stable, and the water movement ~~basically~~ showed an upward movement of soil water in the upper soil layer and a downward movement of soil water in the lower soil layer.

This research mainly studied the second year of the complete maize growth period, and conducted a correlation analysis of the soil water potential in the same growth period before and after two years of the study year. Pearson, Spearman, and Kendall correlation tests were used to verify the correlation. It was found that the soil water potential of maize in the study year at the emergence stage was not correlated with the two years before and after. This may verify the fact that the soil water potential is influenced by external factors such as irrigation and root water uptake during the emergence stage, and that the water movement is more complex and has no regularity. The study year of soil water potential at the flaring and maturation stages showed a significant correlation ($P > 0.01$) with the two years before and after the study year, which indicated that the trend of soil water potential change state in three consecutive years was similar. The analysis shows that at the early stage of crop growth, the soil

http://www.aloki.hu ● ISSN 1589 1623 (Print) ● ISSN 1785 0037 (Online)
DOI: http://dx.doi.org/10.15666/aeer/2004_36313653

water movement state is susceptible to external factors and the soil water movement type is complex. The soil water potential is gradually stabilized as the crop growth period progresses, or due to the stability of crop water demand or other factors; the trend of water potential changes in each growth period is primarily the same. The water potential level is easily affected by external factors such as rainfall and irrigation.

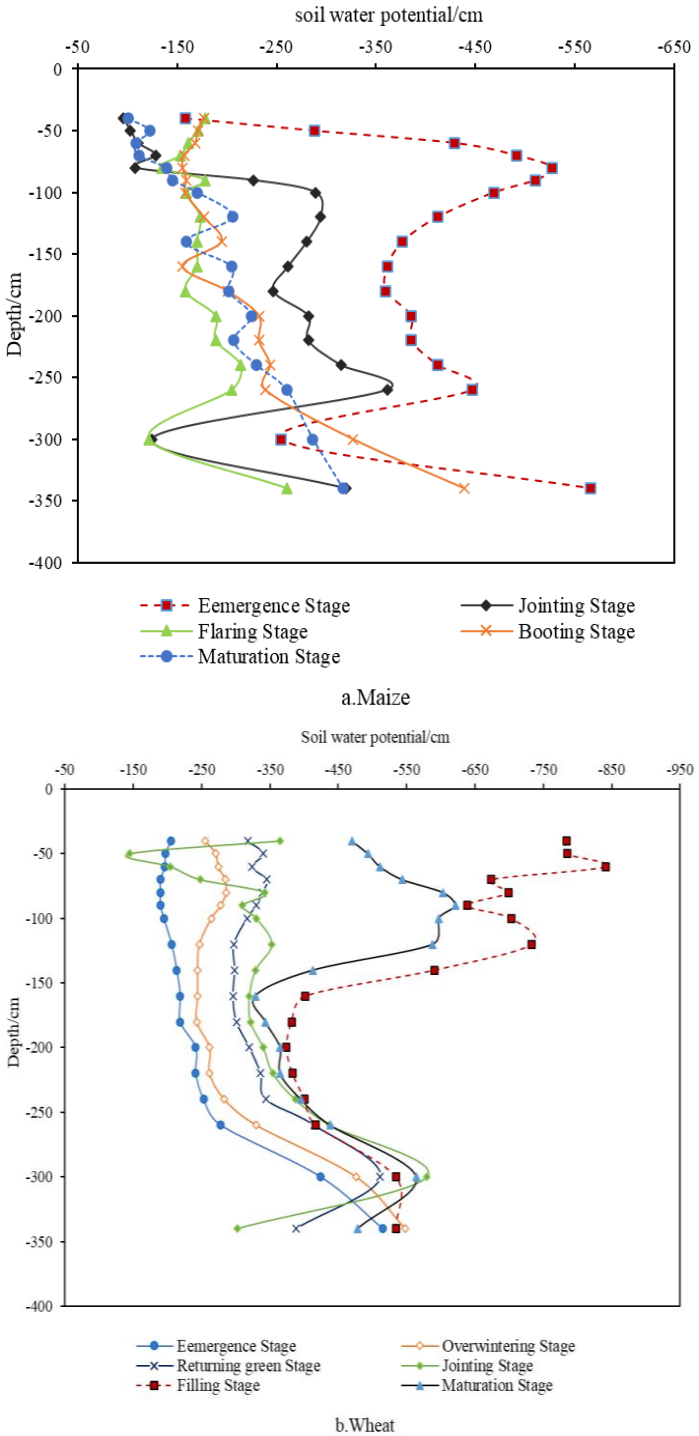

Figure 4. *Water potential migration trends of summer maize and winter wheat in different growth stages*

http://www.aloki.hu ● ISSN 1589 1623 (Print) ● ISSN 1785 0037 (Online)
DOI: http://dx.doi.org/10.15666/aeer/2004_36313653

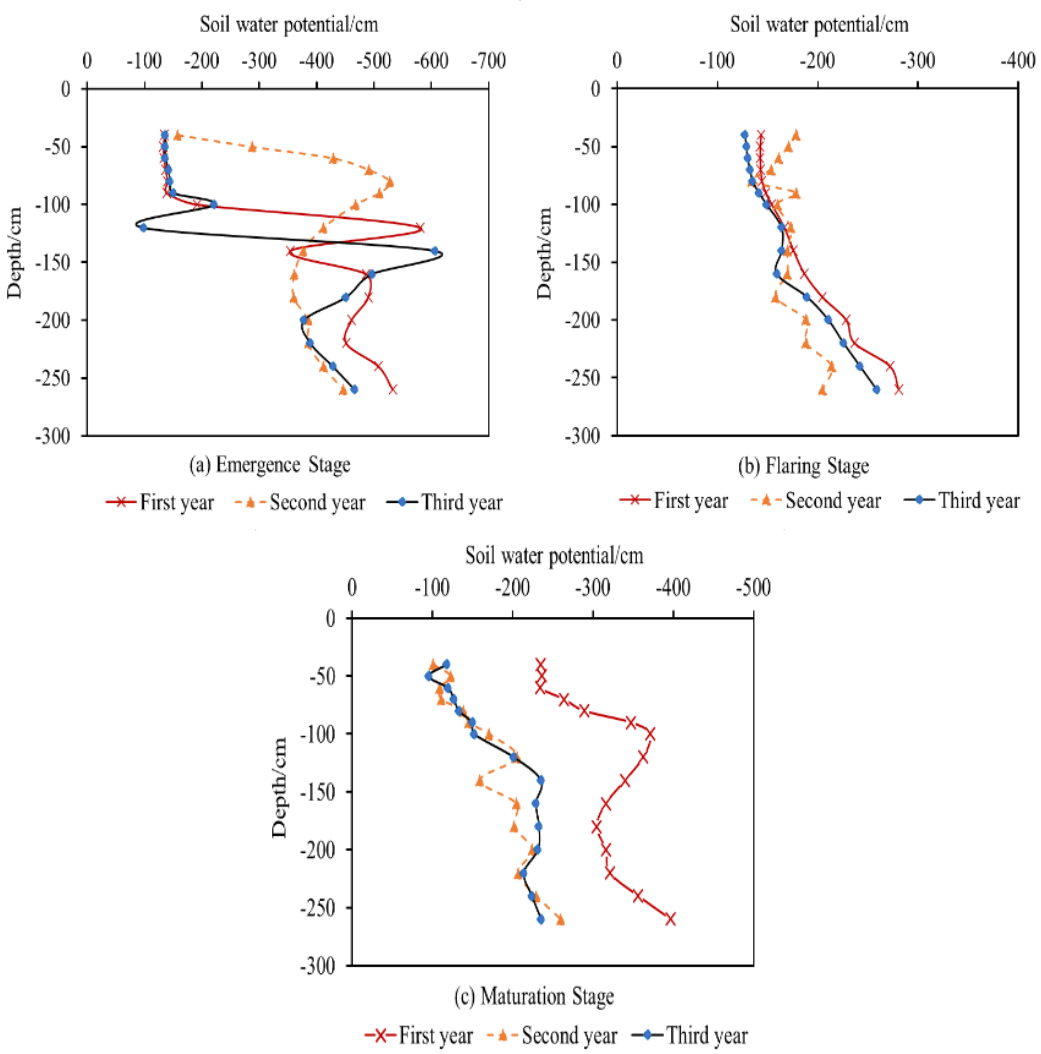

Figure 5. *Comparison of soil water potential dynamics during the same growth period of maize for three consecutive years*

Response of soil moisture movement to precipitation

The above section avoided the time points of precipitation and irrigation when discussing the types of soil moisture movement during the growth period of two crops. This section focuses on the effect of precipitation on soil water movement. A precipitation amount of 52.1 mm was selected to evaluate the effect of precipitation on soil moisture movement by analyzing the change in soil moisture movement type before and after precipitation in the study area.

Figure 6 shows a comparison of the total water potential curves of the soil profile before and after precipitation in the study area. The tendency of soil water movement was the same on day 5 and day 10, and it was considered that the effective impact depth of this precipitation reached 140 cm and the active impact time was 10 days. Therefore, only the movement state changes in soil moisture above 140 cm were discussed. It can be seen from the analysis that the soil water movement above 80 cm is complex and variable in the 5 days before precipitation, which is affected by evaporation and root water uptake, and the soil water movement type is mainly evaporation-infiltration type.

http://www.aloki.hu ● ISSN 1589 1623 (Print) ● ISSN 1785 0037 (Online)
DOI: http://dx.doi.org/10.15666/aeer/2004_36313653

From the day of precipitation to 7 h after precipitation to 1 day after precipitation, a polymeric zero flux surface is formed at 60–100 cm near the surface, and the soil water movement type is infiltration-evaporation-infiltration. After 5 days of precipitation, the aggregated zero flux surface disappeared and the soil moisture movement type gradually turned into an infiltration type. The soil moisture movement type gradually returned to the evaporation-infiltration type after 20 days of precipitation.

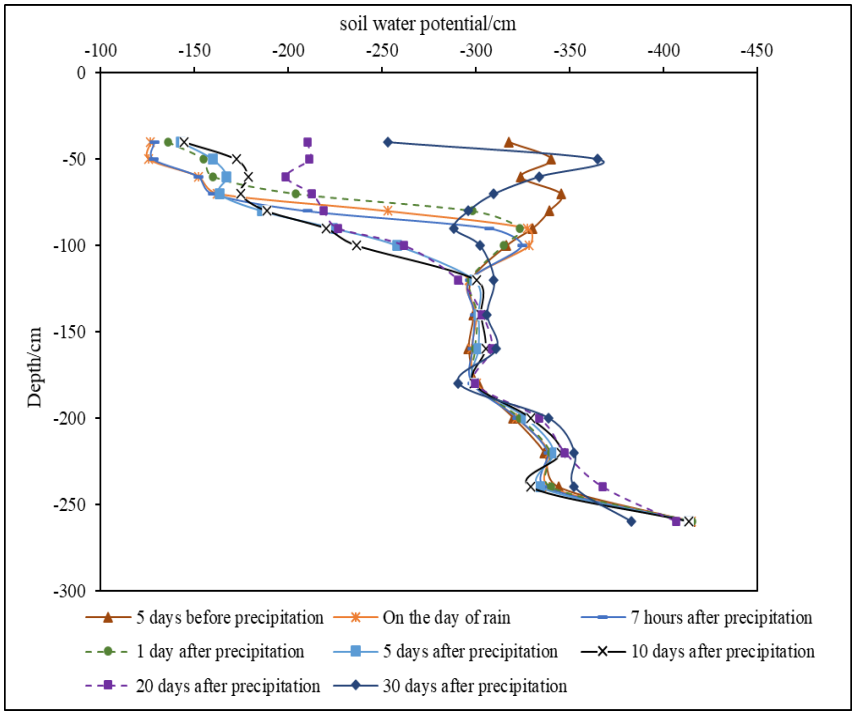

Figure 6. *Characteristics of soil moisture movement before and after a single precipitation*

The statistical analysis of precipitation intensity in the study area from the beginning of April to the end of October was carried out according to the classification criteria of precipitation intensity issued by the National Meteorological Administration. Among the 35 precipitation days, the frequency of light rainfall of 0.1–9.9 mm (27 times) accounted for 77.1%, medium rainfall of 10.0–24.9 mm (five times) accounted for 14.3%, heavy rainfall of more than 25.0–49.9 mm (one time) accounted for 3%, and the frequency of heavy rainfall of more than 50 mm (two times) accounted for 6% of the total rainfall. Therefore, the precipitation in the test area was primarily light rainfall. To reduce the influence of early precipitation on the soil water potential, only the first day of precipitation was considered in this study for precipitation events on consecutive days, and the influence of eight precipitation events on the soil water potential was analyzed.

The variation in soil water potential values (averaged across soil layers) on the 2nd day after precipitation relative to the previous precipitation is shown in *Figure 7*. The impact of soil water potential during a single strong rainfall event reached a depth of 140 cm; there were three precipitation events of less than 10 mm, and the soil water potential varied between 0 and 10 cm. It can be seen that precipitation of less than 10 mm had no significant effect on the soil water potential, which is consumed by the evapotranspiration of the surface soil, while precipitation greater than 10 mm increased the soil water potential. The water potential increased further with greater precipitation.

http://www.aloki.hu ● ISSN 1589 1623 (Print) ● ISSN 1785 0037 (Online)
DOI: http://dx.doi.org/10.15666/aeer/2004_36313653

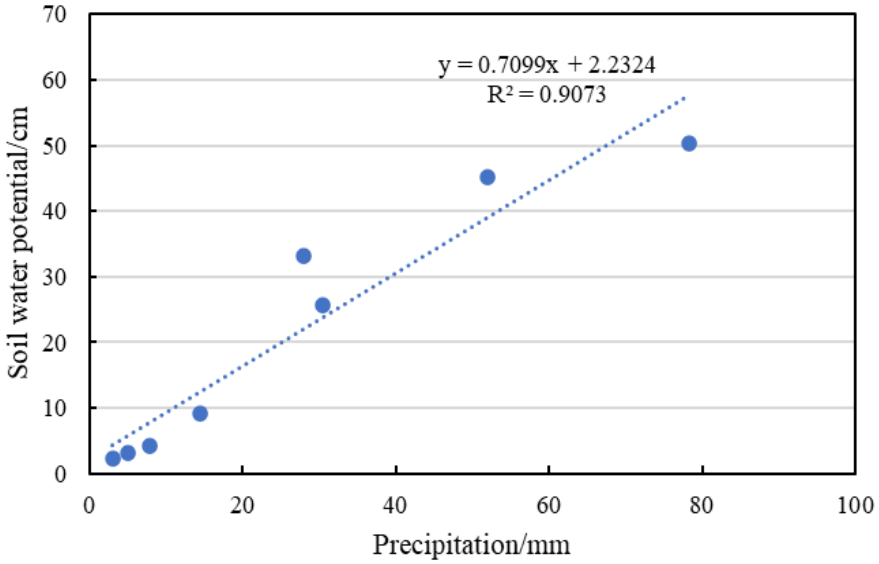

Figure 7. *Response of soil water potential to precipitation*

Potential groundwater recharge

The distribution of the soil profile water potential in the test plots during the study period is shown in *Figure 4*. The soil water potential near the surface is affected by precipitation, irrigation, and evaporation; therefore, it changes significantly. The soil water potential gradient difference is large and the direction of water flow also changes frequently, owing to the zone where the soil water potential gradient changed significantly. In this study, the upper boundary of this zone is the surface and the lower boundary can reach the maximum depth (180 cm) at which the dispersive zero-flux surface develops a downward trend for many years or at least for the entire study period. The soil water potential below the profile is less affected by precipitation, irrigation, and evaporation; therefore, it changes slowly. The difference in the soil water potential gradient is small and the direction of water flow is always downward, owing to the zone where the soil water potential gradient changed slightly. Based on the above principles, the location of the boundary was chosen at a depth of 200 cm from the surface below the deepest zero flux surface, where the direction of soil water movement is always downward; thus, the water flow through this boundary is equivalent to the potential infiltration recharge of precipitation or irrigation water (Wu et al., 2012).

Figure 8 shows the soil water fluxes at 200 cm from the location boundary calculated using *Equations 3*, *4*, and *5*, and demonstrates that the infiltration recharge has a certain relationship with precipitation and irrigation. The infiltration recharge was also large at the time of large precipitation and irrigation volume, but with a certain lag effect, indicating that root leakage still existed under the irrigation quota at that time. It is necessary to alleviate the irrigation quota to reduce deep leakage and improve the utilization efficiency of irrigation water. The infiltration recharge in the absence of rainfall or irrigation is small and it shows irregular fluctuations, which is related to the redistribution of soil moisture after precipitation or irrigation and has some influence on the length of the calculation period.

http://www.aloki.hu ● ISSN 1589 1623 (Print) ● ISSN 1785 0037 (Online)
DOI: http://dx.doi.org/10.15666/aeer/2004_36313653

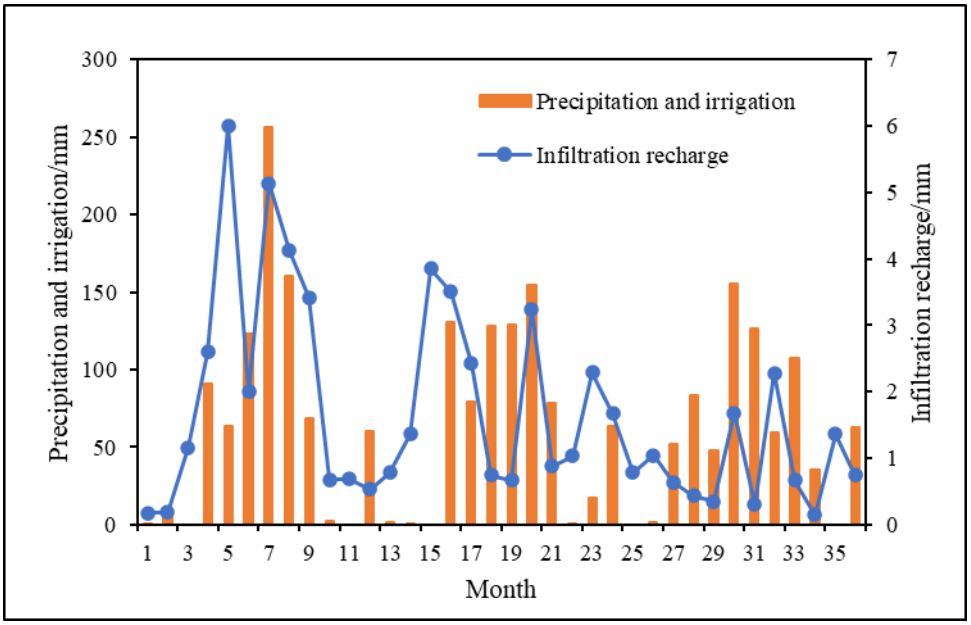

Figure 8. *Cumulative infiltration recharge curve of soil water over time for three consecutive years*

Water balance analysis in the study area

The main infiltration recharge in the study area comes from atmospheric precipitation and irrigation infiltration, and the main water consumption is sourced from surface evaporation and transpiration of crops (without considering the influence of runoff conditions). The North China Plain is an arid and semi-arid area with strong evaporation. The annual evapotranspiration for successive monitoring years can be seen in *Figure 9*, with evapotranspiration being highest in the no-crop period before maize planting, up to 9 mm, due to rainfall and cropping patterns. Transpiration is more intense in the middle and late stages of development in wheat and ~~in~~ the rapid growth stage in maize. The results of the water balance calculations show that the main sources of water recharge to the soil layer in the study area were precipitation (55.68%) and irrigation (44.32%), and the main source of discharge was evapotranspiration (97.89%) (*Table 2*). A few sources (2.11%) are used for groundwater recharge, and some are stored in the soil layer. *Table 2* shows that total evapotranspiration during the reproductive period is wheat > maize > fallow, with wheat requiring more irrigation water. The infiltration recharge is positive in all three years, indicating that the downward infiltration acts as a recharge to groundwater. The soil water in the basin showed a negative equilibrium in the full equilibrium period, indicating that irrigation infiltration recharge does not compensate for evapotranspiration during the continuous monitoring years, and that irrigation practices in the study area are causing some waste.

Discussion

The type of soil moisture movement varies significantly at different growth stages of the crop. In this study, soil moisture dynamics were found to show some regular changes in the profile, which is consistent with the research findings of Tian (2017). The state of change of the water potential is similar to continuous annual monitoring

http://www.aloki.hu ● ISSN 1589 1623 (Print) ● ISSN 1785 0037 (Online)
DOI: http://dx.doi.org/10.15666/aeer/2004_36313653

and can be accurately analyzed by identifying the location of the zero flux surface and the type of soil moisture movement in the study area (Lin et al., 2014; Zhang et al., 2017). Many external factors affect soil moisture dynamics, such as meteorological factors (Sahaar et al., 2020), precipitation (Zhang et al., 2019a), crop type (Yetbarek et al., 2020), and depth of the buried water table (Zhang et al., 2019b). Jiang et al. (2021) analyzed the response of soil water potential to atmospheric precipitation in grasslands from April to October; they observed that precipitation affected soil water potential and increased continuously with rainfall, which is ~~by~~ the conclusion of the present study. After studying the effects of single heavy rainfall and multiple precipitation events on soil water potential, this paper finds that precipitation greater than 10 mm recharges soil water to some extent, The effect of rainfall on soil water transport has a lagging effect, its soil water movement type ~~basically~~ shows a cyclic change characteristic. However, the process of water redistribution in soil and its influence on deep soil water after rainfall is more complicated, and long-term monitoring is needed to elucidate the influence of different rainfall patterns and vegetation root distribution on soil layers at different depths.

Table 2. *Calculation of water balance in the study area (mm*a^{-1})*

Year	Crop types	Replenishment		Discharge		Storage variables
		Precipitation P/(mm*a^{-1})	Irrigation I/(mm*a^{-1})	Evapotranspiration E_T/(mm*a^{-1})	Infiltration recharge Q/(mm*a^{-1})	ΔW/(mm*a^{-1})
First year	Summer maize	305.6	180	291.8	26.7	-141.4
	Winter wheat	92.7	240	519.1		
	No crops	15.1		137.2		
Second year	Summer maize	294.5	134	284.5	22.5	-167.3
	Winter wheat	131.2	180	503.3		
	No crops	43		139.7		
Third year	Summer maize	172.9	120	289	10.5	-164.2
	Winter wheat	122.5	187	515.4		
	No crops	130.3		82		
Total/mm		1307.8	1041	2762	59.6	-472.9
Percentage		55.68%	44.32%	97.89%	2.11%	

Evapotranspiration is an important element in the soil-plant-atmosphere system and plays a vital role in crop growth and development (Bakhshoodeh et al., 2022; Nyawade et al., 2021). Many factors affect the evapotranspiration of crops, including meteorological factors (radiation, sunshine duration, temperature, saturation water-air pressure difference, wind speed, etc.), crop factors (plant height, leaf area, etc.) and soil factors (soil temperature, soil moisture, etc.). The transpiration in this study ranged from 284.5 to 291.8 mm for maize, 503.3 to 519.1 mm for wheat, and 82 to 139.7 mm for soil surface evaporation during the no-crop period. The evapotranspiration of summer maize under different water supply conditions was found to be 285.51-334.18 mm by Yu (2016), which is similar to the conclusions of the study. Irrigation and precipitation were the main sources of water consumed for evapotranspiration in the study area. However, due to the arid climate of the North China Plain, irrigation and rainfall were not sufficient to meet the evapotranspiration demand in a continuous monitoring year. Therefore, the farm management practices and irrigation patterns in the irrigation area were not reasonable.

http://www.aloki.hu ● ISSN 1589 1623 (Print) ● ISSN 1785 0037 (Online)
DOI: http://dx.doi.org/10.15666/aeer/2004_36313653

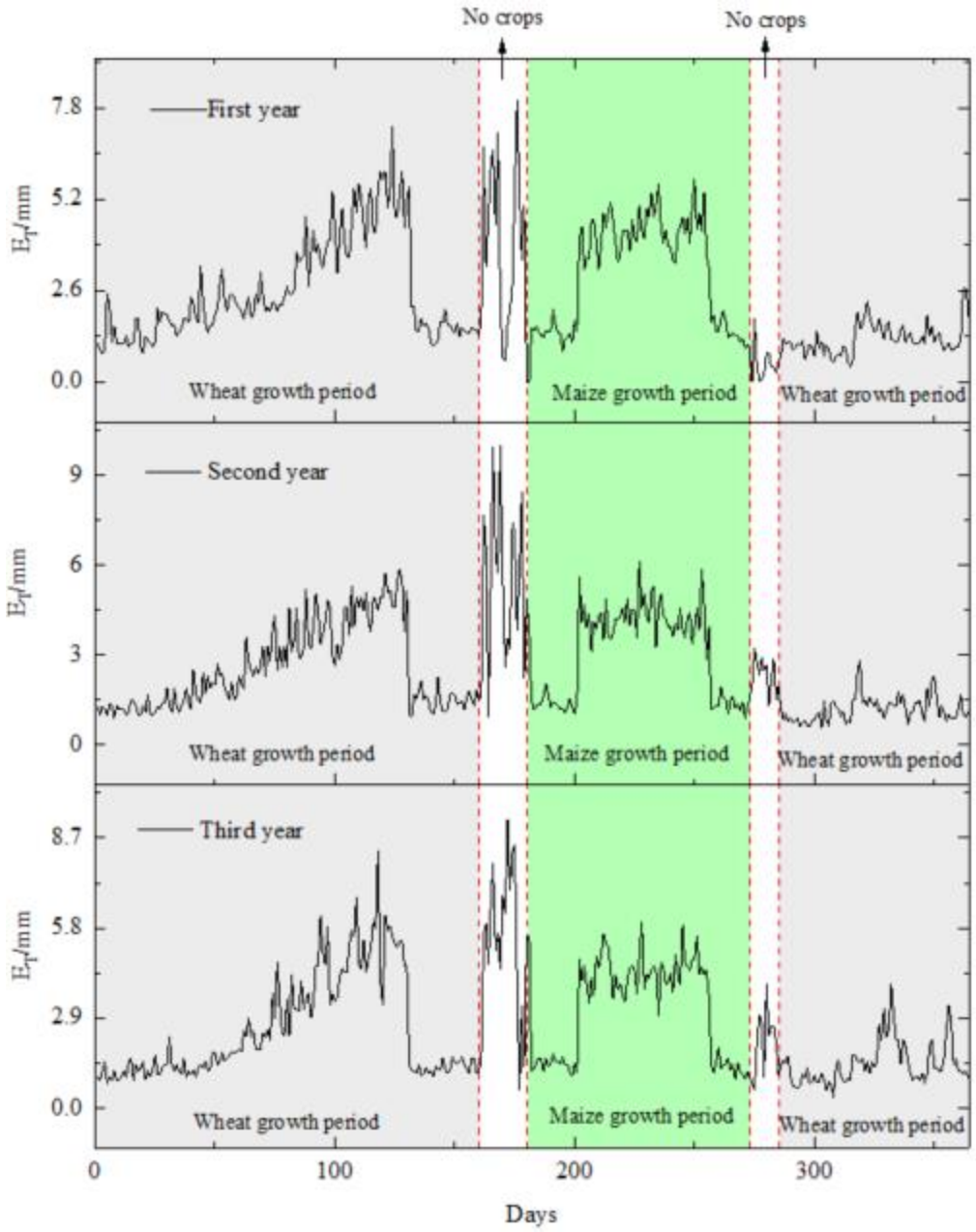

Figure 9. *Annual evapotranspiration for consecutive monitoring years*

The irrigation method used in the irrigation area is heavy irrigation, which can reach 240 mm in the winter wheat crop. The crude irrigation methods had resulted in a significant waste of water, thus affecting the water balance in large buried irrigation areas. The amount of infiltration recharge from precipitation and irrigation in the irrigation area did not compensate for the evapotranspiration discharge. The soil had a negative water storage capacity, but there was a certain amount of vertical infiltration recharge. This indicates that under current irrigation practices, soil water is not being used efficiently and is being wasted, which is one of the reasons for the constant decline in groundwater levels (Cheng et al., 2021). It is still difficult to determine potential infiltration recharge in large buried areas with severe groundwater overdrafts. Kendy et

http://www.aloki.hu ● ISSN 1589 1623 (Print) ● ISSN 1785 0037 (Online)
DOI: http://dx.doi.org/10.15666/aeer/2004_36313653

al. (2004) and Wang et al. (2010) confirmed the existence of vertical recharge in irrigated farmland areas using experiments and numerical simulations to address the question of whether there is vertical recharge on the surface of farmland areas with a large burial depth of groundwater in the North China Plain. According to the above-mentioned research, the upper boundary of the stable zone of soil water potential change at a depth of 200 cm is used as the infiltration boundary of potential infiltration recharge, and finds that there is a certain amount of vertical infiltration recharge of precipitation or irrigation water in the typical irrigation areas of the North China Plain with large depth of burial, but due to the influence of the monitoring depth, this conclusion needs to be verified at a deeper level. However, the conclusion needs to be verified at a deeper level due to the limitation of the monitoring depth.

Conclusion

(1) The distribution of water potential in the soil has obvious zoning characteristics. Shallow soil (0–100 cm) is a strong change in the soil water potential zone, which is vulnerable to rainfall infiltration recharge, evaporation, plant transpiration, and other effects. The soil between 100–200 cm depth was the lagging zone of soil water potential change, and the soil layer was affected by external factors causing changes in the soil water movement state. The soil at the depth of 200–300 cm was the stable zone of soil water potential change, and the soil layer was less affected by precipitation and evaporation. The soil water potential and the soil water movement were relatively stable. The soil layer below 300 cm is called the deep soil water movement zone, which is not affected by external factors such as precipitation and irrigation. However, the soil water potential changes with time and the reason for this phenomenon may be the groundwater level or the effect of the dominant flow of large channels.

There were significant differences in the soil water infiltration status of crops at different growth stages. During the growing period of summer maize, soil water potential trends change significantly and soil water movement becomes more complex and is greatly affected by precipitation; there are generally multiple zero flux surfaces, and the zero-flux surface also decreases as the growing period progresses. The variation trend of soil water potential within the growth period of winter wheat becomes increasingly significant with the warming of weather. The zero-flux surface is easily formed near the ground under the influence of precipitation and irrigation, and the soil movement is mainly dominated by infiltration at the jointing, filling, and maturation stages.

(2) Precipitation greater than 10 mm recharges soil water to some extent. The soil moisture type gradually changes from evaporation-infiltration type before precipitation to infiltration-evaporation-infiltration type at the initial stage of precipitation; it then changes to infiltration type after precipitation, and finally reverts to evaporation-infiltration type after a longer period after precipitation, thus forming a complete cycle. Moreover, during the response of the soil water movement state to precipitation, the position of the zero-flux surface gradually moves down and returns to the position of the zero-flux surface before precipitation, and finally forms the infiltrated soil water state.

(3) In the study on the potential recharge of soil water in the area with a large burial depth of groundwater, the upper boundary of 200 cm of the zone exhibiting a stable soil water potential change was used to study the infiltration recharge of soil water in

http://www.aloki.hu ● ISSN 1589 1623 (Print) ● ISSN 1785 0037 (Online)
DOI: http://dx.doi.org/10.15666/aeer/2004_36313653

Luancheng area. It was found that the infiltration recharge was related to rainfall and irrigation; that is, it increases with a rise in rainfall and irrigation, but it has a certain lag effect.

(4) The main recharge sources of soil moisture in the irrigation area were precipitation (55.68%) and irrigation (44.32%), and the main discharge source was evapotranspiration (98.89%). A few sources (2.11%) were used for groundwater recharge, and the soil water in the basin showed a negative equilibrium in the full equilibrium period.

Acknowledgments. Two anonymous reviewers and my editor are thanked for helpful suggestions on an earlier version of the manuscript. This study was funded by the National Natural Science Foundation of China (41877201) and the Geological Survey Project of China Geological Survey (DD20221676).

Conflict of interests. The authors declare that they have no known competing financial interests or personal relationships that could have appeared to influence the work reported in this paper.

REFERENCES

[1] Adhikari, B., Wang, L. (2020): The potential contribution of soil moisture to fog formation in the Namib Desert. – J Hydrol 591: 125326. https://doi.org/10.1016/j.jhydrol.2020.125326.

[2] Allen, R. G., Pereira, L. S., Raes, D., Smith, M. (1998): Crop Evapo-Transpiration: Guidelines for Computing Crop Water Requirements. – United Nations Food and Agriculture Organization, Irrigation and Drainage Paper No. 56. FAO, Rome.

[3] Ayantobo, O. O., Wei, J. (2019): Appraising regional multi-category and multi-scalar drought monitoring using standardized moisture anomaly index (SZI): A water-energy balance approach. – J Hydraul 579: 124139. https://doi.org/10.1016/j.jhydrol.2019.124139.

[4] Bakhshoodeh, R., Ocampo, C., Oldham, C. (2022): Evapotranspiration rates and evapotranspirative cooling of green façades under different irrigation scenarios. – Energy and Buildings 112223. https://doi.org/10.1016/j.enbuild.2022.112223.

[5] Cheng, Z. S., Su, C., Zheng, Z. X., Chen, Z. Y., Wei, W. (2021): Characterize groundwater vulnerability to intensive groundwater exploitation using tritium time-series and hydrochemical data in Shijiazhuang, North China Plain. – Journal of Hydrology. 603: 126953. DOI: 10.1016/j.jhydrol.2021.126953.

[6] Dias, A. S., Pirone, M., Nicotera, M. V., Urciuoli, G. (2021): Hydraulic characterization of an unsaturated vegetated soil: the role of plant roots and hydraulic hysteresis. – Geomech Energy Envir 100235. https://doi.org/10.1016/j.gete.2021.100235.

[7] Han, S. P., Jing, J. H., Sun, J. C., Shi, Y. C., Wang, S. (2005): Analyses of moisture movement Types and movement mechanism of moisture and salinity at soil section. – J Agro-Environ Sci (S1): 148-152. https://kns.cnki.net/kcms/detail/detail.aspx?FileName=NHBH2005S1034&DbName=CJFQ2005.

[8] Hu, X. Y., Lei, H. M. (2021): Fifteen-year variations of water use efficiency over a wheat-maize rotation cropland in the North China Plain. – Agr Forest Meteorol 306: 108430. https://doi.org/10.1016/j.agrformet.2021.108430.

[9] Hu, C., Saseendran, S. A., Green, T. R., Ma, L., Li, X., Ahuja, L. R. (2006): Evaluating nitrogen and water management in a double-cropping system using RZWQM. – Vadose Zone Journal 5(1): 493-505. https://doi.org/10.2136/vzj2005.0004.

http://www.aloki.hu ● ISSN 1589 1623 (Print) ● ISSN 1785 0037 (Online)
DOI: http://dx.doi.org/10.15666/aeer/2004_36313653

[10] Huang, X. J., Wang, H. F., Zhang, M., Horn, R., Ren, T. (2021): Soil water retention dynamics in a Mollisol during a maize growing season under contrasting tillage systems. – Soil Till Res 209: 104953. https://doi.org/10.1016/j.still.2021.104953.
[11] Jia, X. Y., O'Connor, D., Hou, D. Y., Jin, Y. L., Li, G. H., Zheng, C. M., Ok, Y. S., Tsang, D. C., Luo, J. (2019): Groundwater depletion and contamination: spatial distribution of groundwater resources sustainability in China. – Sci Total Environ 672: 551-562. https://doi.org/10.1016/j.scitotenv.2019.03.457.
[12] Jiang, Z. C., Jiang, Z. R., Zhao, W. J., Liao, K. T., Luo, Y. M., Feng, J. Y. (2021): Study on the variation characteristics of grassland vegetation soil water potential in Xishui Forest Area of Qilian Mountains, Gansu. – J Southwest Forestry Univ (Nat Sci) 41(2): 177-181. https://kns.cnki.net/kcms/detail/53.1218.S.20200829.1234.002.html.
[13] Jing, E. C., Fei, J., Zhang, X. H. (1994): Experimental Study on Soil Water Flux Method. – Earthquake Publishing, Beijing.
[14] Joly, F., Weibel, A. K., Coulis, M., Throop, H. L. (2019): Rainfall frequency, not quantity, controls isopod effect on litter decomposition. – Soil Biol Biochem 135: 154-62. https://doi.org/10.1016/j.soilbio.2019.05.003.
[15] Ju, Z. Q., Li, X. X., Hu, C. S. (2015): Water dynamics and groundwater recharge in a deep vadose zone. – Water Science and Technology: Water Supply 16(3): 579-586. https://doi.org/10.2166/ws.2015.165.
[16] Kamal, E. G. M., Abdelaty, D., Moubark, K., Abdelkareem, M. (2021): Assessment of the groundwater possibility and its efficiency for irrigation purposes in the area east of Qena, Egypt. – Arab J Geosci 14(10): 839. https://doi.org/10.1007/s12517-021-07041-2.
[17] Kassaye, K. T., Boulange, J., Lam, V. T., Saito, H., Watanabe, H. (2020): Monitoring soil water content for decision supporting in agricultural water management based on critical threshold values adopted for Andosol in the temperate monsoon climate. – Agr Water Manage 229: 105930. https://doi.org/10.1016/j.agwat.2019.105930.
[18] Kendy, E., Zhang, Y., Liu, C., Wang, J., Steenhuis, T. (2004): Groundwater recharge from irrigated cropland in the North China Plain: case study of Luancheng County, Hebei Province, 1949-2000. – Hydrol Process 18(12): 2289-302. https://doi.org/10.1002/hyp.5529.
[19] Kristo, C., Rahardjo, H., Satyanaga, A. (2019): Effect of hysteresis on the stability of residual soil slope. – Int Soil Water Conse 7(3): 226-38. https://doi.org/10.1016/j.iswcr.2019.05.003.
[20] Li, M., He, Y. J., Lin, W. J., Wang, G. L. (2014): Research on soil moisture transport mechanism in the piedmont of the Taihang Mountain. – J Arid Land Resour Environ 28(3): 101-106. http://dx.chinadoi.cn/10.13448/j.cnki.jalre.2014.03.016.
[21] Li, P., Xu, H. L., Pan, Y., Sun, Y., Wang, X. J. (2017): A comparative study on precipitation infiltration recharge calculation methods for Beijing Plain. – J China Hydrol 37(2): 31-35. https://kns.cnki.net/kcms/detail/detail.aspx?FileName=SWZZ201702006&DbName=CJFQ2017.
[22] Li, H. T., Li, L., Liu, N., Chen, S. Y., Shao, L. W., Sekiya, N., Zhang, X. Y. (2022): Root efficiency and water use regulation relating to rooting depth of winter wheat. – Agricultural Water Management 269: 107710. https://doi.org/10.1016/j.agwat.2022.107710.
[23] Lin, D., Jin, M. G., Ma, B., Wang, B. G. (2014): Characteristics of infiltration recharge at thickening vadose zone using soil hydraulic parameters. – Earth Sci 39(6): 760-768. https://kns.cnki.net/kcms/detail/detail.aspx?FileName=DQKX201406011&DbName=CJFQ2014.
[24] Lu, C. P., Song, Z. Y., Wang, W. J., Zhang, Y., Si, H. Y., Liu, B., Shu, L. C. (2021): Spatiotemporal variation and long-range correlation of groundwater depth in the Northeast China Plain and North China Plain from 2000~2019. – J Hydrol-Reg Stud 37: 100888. https://doi.org/ 10.1016/j.ejrh.2021.100888.

http://www.aloki.hu ● ISSN 1589 1623 (Print) ● ISSN 1785 0037 (Online)
DOI: http://dx.doi.org/10.15666/aeer/2004_36313653

[25] Muhammad, E. S., Ibrahim, M. M., El-Sayed, A. (2021): Effects of drain depth on crop yields and salinity in subsurface drainage in Nile Delta of Egypt. – Ain Shams Eng J. https://doi.org/10.1016/j.asej.2021.01.008.
[26] Nyawade, S. O., Gitari, H. I., Karanja, N. N., Gachene, C. K. K., Schulte-Geldermann, E., Parker, M. L. (2021): Yield and evapotranspiration characteristics of potato-legume intercropping simulated using a dual coefficient approach in a tropical highland. – Field Crops Research 274: 108327. https://doi.org/10.1016/j.fcr.2021.108327.
[27] Ordóñez, R. A.., Castellano, M. J., Hatfield, J. L., Helmers, M. J., Licht, M. A., Liebman, M., Dietzel, R., Martinez-Feria, R., Iqbal, J., Puntel, L. A., Córdova, S. C., Togliatti, K., Wright, E. E., Archontoulis, S. V. (2018): Maize and soybean root front velocity and maximum depth in Iowa, USA. – Field Crops Research 215: 122-131. https://doi.org/10.1016/j.fcr.2017.09.003.
[28] Pei, Y. S., Li, X. D., Zhao, Y., Zhai, J. Q. (2020): Research on vertical recharge and specific yield of the unconfined aquifer in a typical deep groundwater areas of North China Plain. – South-to-North Water Tran Sci Technol 18(1): 176-193. http://dx.chinadoi.cn/10.13476/j.cnki.nsbdqk.2020.0019.
[29] Pereira, L. S., Paredes, P., Jovanovic, N. (2020): Soil water balance models for determining crop water and irrigation requirements and irrigation scheduling focusing on the FAO56 method and the dual Kc approach. – Agr Water Manage 241: 106357. https://doi.org/10.1016/j.agwat.2020.106357.
[30] Pullens, J. W. M., Sørensen, C. A. G., Olesen, J. E. (2021): Temperature-based prediction of harvest date in winter and spring cereals as a basis for assessing viability for growing cover crops. – Field Crop Res 264: 108085. https://doi.org/10.1016/j.fcr.2021.108085.
[31] Sahaar, S. A., Niemann, J. D. (2020): Impact of regional characteristics on the estimation of root-zone soil moisture from the evaporative index or evaporative fraction. – Agr Water Manage 238: 106225. https://doi.org/10.1016/j.agwat.2020.106225.
[32] Shen, Y. J., Min, L. L., Wu, L., Shen, Y. J., Li, H. J., Zhang, G. L. (2021): Functions and applications of critical zone observatory of Luancheng agro-ecosystem experimental station, Chinese Academy of Sciences (Luancheng Critical Zone Observatory). – Bulletin of Chinese Academy of Sciences 36(4): 502-511. https://doi.org/10.16418/j.issn.1000-3045.20210407001.
[33] Tian, Y. (2017): Dynamic Characteristics of Soil Water Potential in Larch Forest in Growing Season. – Inner Mongolia Agricultural University, Hohhot.
[34] Vermeire, L. T., Rinella, M. J. (2020): Fall water effects on growing season soil water content and plant productivity. – Rangeland Ecol Manag 73(2): 252-8. https://doi.org/10.1016/j.rama.2019.11.006.
[35] Wang, S. X., Zhou, J. L., Yu, F., Dong, X. G. (2005): Application of HYDRUS-1D model to evaluating soil water resource. – Research of Soil and Water Conservation 2: 36-38.
[36] Wang, B. G., Jin, M. G., Wang, G. L. (2010): Effects of straw mulch on soil water in cropland. – China Rural Water Hydropower 6: 76-80+84. https://kns.cnki.net/kcms/detail/detail.aspx?FileName=ZNSD201006024&DbName=CJFQ2010.
[37] Wei, W., Chen, Z. Y. (2017): The effects of climate change on potential groundwater recharge - a case study of Luancheng experimental station 15(5): 29-35. – https://doi.org/10.13476/j.cnki.nsbdqk.2017.05.005.
[38] Wu, Q. H., Wang, G. L., Lin, W. J., Zhang, F. W. (2012): Estimating Groundwater Recharge of Taihang Mountain Piedmont in Luancheng County, Hebei Province, China. – Bulletin of Geological Science and Technology 31(2): 99-105. http://10.3969/j.issn.1000-7849.2012.02.016.
[39] Xiao, D. P., Liu, D. L., Feng, P. Y., Wang, B., Waters, C., Shen, Y. J., Qi, Y. Q., Bai, H. Z., Tang, J. Z. (2021): Future climate change impacts on grain yield and groundwater use

http://www.aloki.hu ● ISSN 1589 1623 (Print) ● ISSN 1785 0037 (Online)
DOI: http://dx.doi.org/10.15666/aeer/2004_36313653

under different cropping systems in the North China Plain. – Agr Water Manage 246: 106685. https://doi.org/10.1016/j.agwat.2020.106685.

[40] Xu, F., Liu, Y. L., Du, W. C., Li, C. L., Xu, M. L., Xie, T. C., Yin, Ying, Guo, H. Y. (2021): Response of soil bacterial communities, antibiotic residuals, and crop yields to organic fertilizer substitution in North China under wheat–maize rotation. – Sci Total Environ 785: 147248. https://doi.org/10.1016/j.scitotenv.2021.147248.

[41] Yetbarek, E., Kumar, S., Ojha, R. (2020): Effects of soil heterogeneity on subsurface water movement in agricultural fields: a numerical study. – J Hydrol 590: 125420. https://doi.org/10.1016/j.jhydrol.2020.125420.

[42] Yu, L. Y. (2016): Simulation of Water and Heat Transfer in SPAC System for Summer Maize Under Conditions of Different Water Supply. – Northwest A&F University, Yangling.

[43] Zhang, G. H., Fei, Y. H., Shen, J. M., Yang, L. Z. (2007): Influence of unsaturated zone thickness on precipitation infiltration for recharge of groundwater. – J Hydraul Eng 5: 611-617. https://kns.cnki.net/kcms/detail/detail.aspx?FileName=SLXB200705015&DbName=CJFQ2007.

[44] Zhang, S. Y., Shu, L. C., Min, X., Hu, H. J., Zou, Z. K. (2017): Calculation of precipitation infiltration recharge based on land-use type. – J Jilin Univ (Earth Sci Edit) 47(3): 860-867. http://dx.chinadoi.cn/10.13278/j.cnki.jjuese.201703206.

[45] Zhang, H., Li, Y., Meng, Y. L., Cao, N., Li, D. S., Zhou, Z. G., Chen, B. L., Dou, F. G. (2019a): The effects of soil moisture and salinity as functions of groundwater depth on wheat growth and yield in coastal saline soils. – J Integr Agr 18(11): 2472-2482. https://doi.org/10.1016/S2095-3119(19)62713-9.

[46] Zhang, J., Little, D. N., Hariharan, N., Kim, Y. R. (2019b): Prediction of climate specific vertical movement of pavements with expansive soils based on long-term 2D numerical simulation of rainwater infiltration. – Comput Geotech 115: 103172. https://doi.org/10.1016/j.compgeo.2019.103172.

[47] Zhang, Y. L., Wu, Z. Y., Singh, V. P., He, H., He, J., Yin, H., Zhang, Y. X. (2021): Coupled hydrology-crop growth model incorporating an improved evapotranspiration module. – Agr Water Manage 246: 106691. https://doi.org/10.1016/j.agwat.2020.106691.

http://www.aloki.hu ● ISSN 1589 1623 (Print) ● ISSN 1785 0037 (Online)
DOI: http://dx.doi.org/10.15666/aeer/2004_36313653